Acta Crystallographica Section B
Structural Science
ISSN 0108-7681

First bent form for the hydroxo-bridged *cis*-diammineplatinum(II) dimer $[Pt_2(NH_3)_4(\mu\text{-}OH)_2](ClO_4)_2$

Ken Sakai,* Yosuke Konno, Noboru Takayama and Satoru Takahashi

Department of Applied Chemistry, Faculty of Science, Tokyo University of Science, Kagurazaka 1-3, Shinjuku-ku, Tokyo 162-8601, Japan

Correspondence e-mail: ksakai@rs.kagu.tus.ac.jp

Received 3 December 2003
Accepted 26 February 2004

The third crystal structure containing the hydroxo-bridged *cis*-diammineplatinum(II) dimer has been determined for a perchlorate salt of the complex, $[Pt_2(NH_3)_4(\mu\text{-}OH)_2](ClO_4)_2$. However, the dinuclear cations in the nitrate and the carbonate salts, $[Pt_2(NH_3)_4(\mu\text{-}OH)_2](NO_3)_2$ [Faggiani, Lippert, Lock & Rosenberg (1977). *J. Am. Chem. Soc.* **99**, 777–781] and $[Pt_2(NH_3)_4(\mu\text{-}OH)_2](CO_3)\cdot H_2O$ [Lippert, Lock, Rosenberg & Zvagulis (1978). *Inorg. Chem.* **17**, 2971–2975], were reported to possess a nearly planar geometry. The cation in the title perchlorate salt has been found to possess an exceptional bent form in which two Pt coordination planes within the dimer are tilted at an angle of 151.7 (1)° to one another. The diplatinum entity has a *syn* orientation with regard to the conformation of two hydroxo bridges, in part due to the one-dimensional hydrogen-bonding network achieved in the crystal structure. DFT MO investigations have also been carried out to reveal that the planar-bent selection could be induced by the *anti–syn* selection at the H(hydroxo) atoms. Comparison has also been made between the geometrical features of the three salts from the viewpoint of the orientation of H(hydroxo) atoms.

1. Introduction

We have thus far succeeded in the development of ‘dimer-based’ one-dimensional platinum chain compounds (Sakai *et al.*, 1998, 2002). In these studies homo-valent and mixed-valent carboxylate-bridged *cis*-diammineplatinum dimers $[Pt_2(NH_3)_4(\mu\text{-carboxylato})_2]^{2+}$ (carboxylate = acetate, propionate *etc.*) have been found to afford one-dimensional platinum chain structures. In these crystal structures the dimer–dimer associations are stabilized with quadruple hydrogen bonds as well as metal–metal bonds formed between the dinuclear entities that are stacked in a one-dimensional fashion. During the course of these studies we found that the diplatinum unit in the title compound, $[Pt_2(NH_3)_4(\mu\text{-}OH)_2](ClO_4)_2$ (I), gives a related one-dimensional framework primarily based on the hydrogen-bonding associations in the crystal structure. More interestingly, it is also found that the diplatinum cation involved in (I) has an exceptional ‘bent’ structure. Previously, a nitrate and a carbonate salt of the complex, $[Pt_2(NH_3)_4(\mu\text{-}OH)_2](NO_3)_2$ [abbreviated as (II); Faggiani *et al.*, 1977] and $[Pt_2(NH_3)_4(\mu\text{-}OH)_2](CO_3)\cdot 2H_2O$ [abbreviated as (III); Lippert *et al.*, 1978], have been structurally determined by X-ray diffraction. In each salt, the diplatinum unit has been

© 2004 International Union of Crystallography
Printed in Great Britain – all rights reserved

Table 1
Experimental details for (I).

Crystal data	
Chemical formula	$Cl_2H_{14}N_4O_{10}Pt_2$
M_r	691.23
Cell setting, space group	Orthorhombic, $P2_12_12_1$
a, b, c (Å)	7.3422 (4), 12.9876 (7), 13.9429 (8)
V (Å^3)	1329.56 (13)
Z	4
D_x (Mg m^{-3})	3.453
Radiation type	Mo $K\alpha$
No. of reflections for cell parameters	4531
θ range (°)	2.9–28.1
μ (mm^{-1})	21.47
Temperature (K)	296 (2)
Crystal form, colour	Needle, pale yellow
Crystal size (mm)	0.2 × 0.10 × 0.06
Data collection	
Diffractometer	Bruker SMART APEX CCD area detector diffractometer
Data collection method	ω scans
Absorption correction	Multi-scan (based on symmetry-related measurements) (*SADABS*; Sheldrick, 1996)
T_{min}	0.069
T_{max}	0.264
No. of measured, independent and observed reflections	7867, 2898, 2726
Criterion for observed reflections	$I > 2\sigma(I)$
R_{int}	0.040
θ_{max} (°)	27.1
Range of h, k, l	$-9 \Rightarrow h \Rightarrow 9$ $-16 \Rightarrow k \Rightarrow 12$ $-15 \Rightarrow l \Rightarrow 17$
Refinement	
Refinement on	F^2
$R[F^2 > 2\sigma(F^2)]$, $wR(F^2)$, S	0.024, 0.056, 0.98
No. of reflections	2898
No. of parameters	168
H-atom treatment	Constrained to parent site
Weighting scheme	$w = 1/[\sigma^2(F_o{}^2)]$
$(\Delta/\sigma)_{max}$	<0.0001
$\Delta\rho_{max}$, $\Delta\rho_{min}$ (e Å^{-3})	1.21, −1.23
Extinction method	*SHELXL*
Extinction coefficient	0.00081 (8)
Absolute structure	Flack (1983), 1361 Friedel pairs
Flack parameter	0.012 (12)

Computer programs: *SMART* (Bruker, 2001), *SAINT* (Bruker, 2001), *SHELXS*97 (Sheldrick, 1997), *SHELXL*97 (Sheldrick, 1997), *KENX* (Sakai, 2002), *TEXSAN* (Molecular Structure Corporation, 2001), *ORTEP*II (Johnson, 1976).

ascertained to possess a planar geometry. Here we report the crystal structure of (I) as the first experimental evidence revealing the existence of a bent form for the $[Pt_2(NH_3)_4(\mu\text{-}OH)_2]^{2+}$ cation. In addition, we report the results of DFT calculations which have been carried out to better understand the conformational properties of this compound. It should also be noted that the present study must be viewed as related to the theoretical investigations of Aullön *et al.* (1998, 2000), in which planar-bent isomerism on the related single-atom-bridged dinuclear complexes were reported. Moreover, it must also be emphasized that the $[Pt_2(NH_3)_4(\mu\text{-}OH)_2]^{2+}$ dimer is one of the possible reaction products in aqueous media of *cis*-$PtCl_2(NH_3)_2$ (cisplatin or *cis*-DDP), which is well known as an efficient anticancer drug (Jamieson & Lippard, 1999).

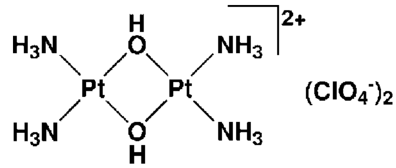

(I)

2. Experimental

2.1. Synthesis of $[Pt_2(NH_3)_4(\mu\text{-}OH)_2](ClO_4)_2$

A solution of *cis*-$PtCl_2(NH_3)_2$ (1 mmol) and $AgClO_4$ (2 mmol) in H_2O (7 ml) was stirred at 343 K for 3 h in the dark, followed by filtration to remove the AgCl precipitated. The pH of the filtrate was then adjusted to 4.0 using aqueous 0.5 *M* NaOH solution. The resulting solution was heated at 313 K for 2 h without stirring. Allowing the solution to stand at 278 K for 1–2 d afforded (I) as pale yellow needles (yield 25%). Analysis: calculated for $Cl_2H_{14}N_4O_{10}Pt_2$: H 2.04, N 8.11; found: H 1.84, N 7.61%.

2.2. X-ray crystallography

A diffraction-quality single crystal of (I) was mounted on a glass fibre. Diffraction data were measured on a Bruker SMART APEX CCD area-detector diffractometer with graphite-monochromated Mo $K\alpha$ radiation (λ = 0.71073 Å). A hemisphere of data was collected in 10 s frames using ω scans of 0.3° per frame. Data reduction was performed with *SAINT* (Bruker, 2001), which *inter alia* applies corrections for Lorentz and polarization effects. Absorption corrections were applied using *SADABS* (Sheldrick, 1996) and the space-group possibilities determined using *XPREP* in *SAINT* (Bruker, 2001). Other details of unit-cell dimensions, data collection and refinement are summarized in Table 1, together with details of the software employed.[1]

The intensity statistics suggested a non-centrosymmetric space group for (I) and $P2_12_12_1$ was assigned on the basis of the systematic absences. The absolute structure was determined from the value of the refined Flack (1983) parameter. H(ammine) atoms were located at their idealized positions and refined as riding atoms with N—H 0.89 Å and $U_{iso}(H) = 1.5U_{eq}(N)$. H(hydroxo) atoms were not located. In the final difference-Fourier synthesis only one residual peak above 1 e Å^{-3} was observed, at 0.64 Å from Pt1. The deepest hole was located 0.95 Å from Pt1.

2.3. DFT calculations

In order to better understand the conformational properties of the $Pt_2(\mu\text{-}OH)_2$ core, we used the density functional theory (DFT) method implemented in the *Gaussian*98 suite of

[1] Supplementary data for this paper are available from the IUCr electronic archives (Reference: BM5007). Services for accessing these data are described at the back of the journal.

programs (Frisch *et al.*, 1998). All calculations were carried out using the B3LYP method which uses hybrid Becke's three-parameter exchange functional (Becke, 1993) with the correlation energy functional of Lee *et al.* (1988). Calculations were performed using the standard double-ζ type LanL2DZ basis set (Dunning & Hay, 1976; Hay & Wadt, 1985*a*; Wadt & Hay, 1985) implemented in *Gaussian*98, without any additional polarization or diffuse functions. The LanL2DZ basis set also uses relativistic effective core potentials (RECP) for the Pt atoms to account for the scalar relativistic effects of the inner 60 core electrons, [Kr]$4d^{10}4f^{14}$ (Hay & Wadt, 1985*b*).

As previously reported by Aullön *et al.* (2000), five possible conformers illustrated in Fig. 1 were constructed as the initial structures for the geometry optimization studies. The initial structures for the planar forms with an *anti* and a *syn* configuration (*pa* and *ps* in Fig. 1) were based on the crystal structure of the nitrate salt $[Pt_2(NH_3)_4(\mu\text{-}OH)_2](NO_3)_2$ (II) (Faggiani *et al.*, 1977). The initial structures for three different bent forms (*ba*, *be* and *bx* in Fig. 1) were constructed based on the crystal structure of the title perchlorate salt $[Pt_2(NH_3)_4(\mu\text{-}OH)_2](ClO_4)_2$ (I). Structures were fully optimized without applying any structural restraints.

3. Results and discussion

3.1. Description of the structure of (I)

As shown in Fig. 2, a dinuclear cation and two perchlorate anions comprise the asymmetric unit of (I). Selected bond distances and angles are summarized in Table 2. Although the coordinate bond distances in (I) are all similar to those reported for (II) and (III), the corresponding valence angles in (I) are slightly different owing to the bent nature of the complex (see Table 2). Two perchlorate anions are associated with the dimer cation through the hydrogen bonds formed between the O atoms of perchlorates and the hydroxo/ammine ligands [O1···O4 2.814 (9), O2···O8 2.891 (8) and N4···O9 2.990 (9) Å]. As shown in Fig. 2(*b*), the two ClO_4^- ions are shifted toward the upper side of a mean plane defined by eight non-H atoms within the dinuclear cation. This indicates that the two H(hydroxo) atoms, whose locations were not clearly determined, must be oriented upward in Fig. 2(*b*) so that they can achieve appropriate hydrogen-bonding interactions with the perchlorate O atoms. This conformation corresponds to the *be* form defined in Fig. 1, an assignment which will be further supported by the interionic hydrogen-bonding geometry described below. The most remarkable feature is that the two Pt coordination planes within the dinuclear cation are inclined by 151.7 (1)° to one another (see Fig. 2*c*). In (II) and (III) the diplatinum entities have a nearly planar geometry [180° for (II), see also Fig. 3; 176.8 (5)° for (III), see also Fig. 4]. As a result, the intracation Pt···Pt distance in (I) [Pt1···Pt2 3.0421 (4) Å] is *ca* 0.05 Å shorter than those in (II)

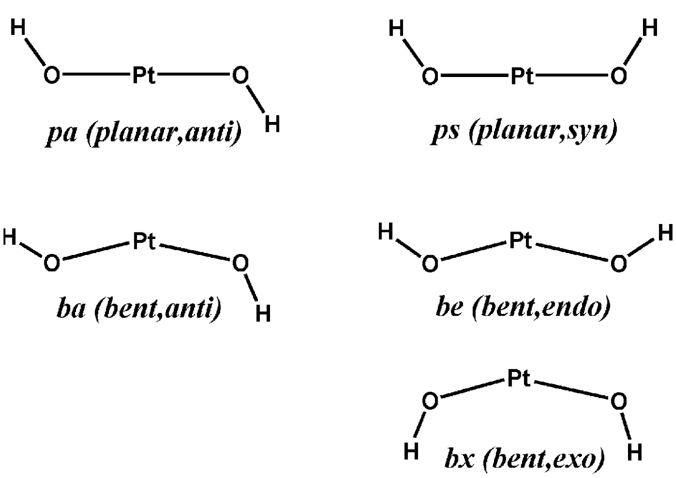

Figure 1
Definition of five possible conformers for the $[Pt_2(NH_3)_4(\mu\text{-}OH)_2]^{2+}$ cation, where all the structures are viewed along the Pt···Pt vector and the ammines are omitted for clarity.

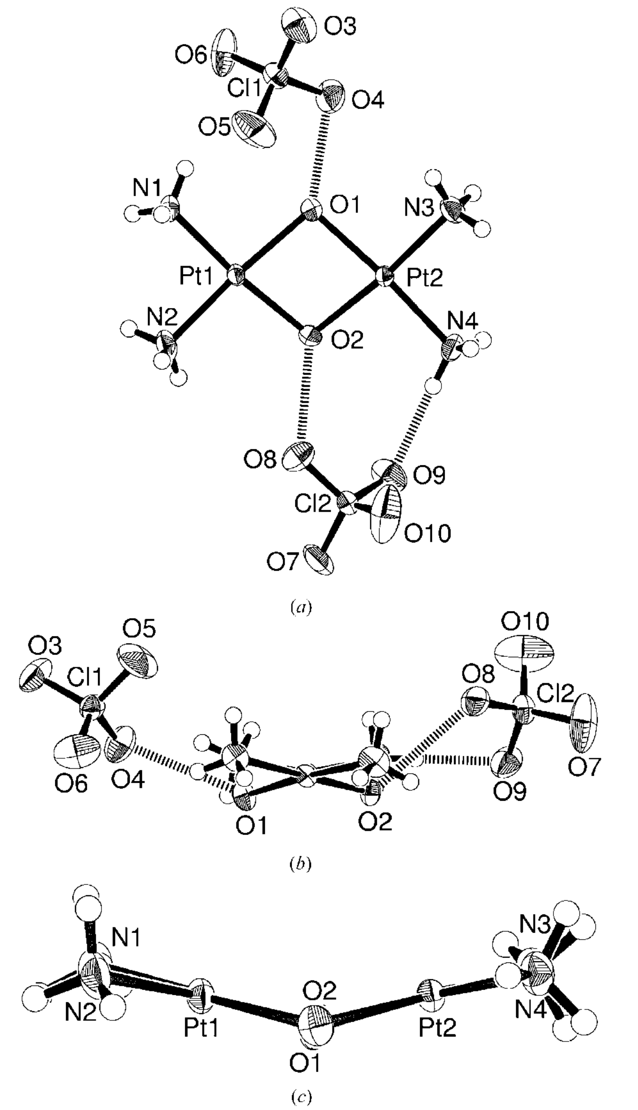

Figure 2
(*a*) A top view, (*b*) a side view along the Pt···Pt vector and (*c*) a side view perpendicular to the Pt···Pt vector for the contents of the asymmetric unit of (I), showing the atom-labelling scheme. Displacement ellipsoids are shown at the 50% probability level. In (*c*) the perchlorate anions are omitted for clarity.

Table 2
Comparison of the geometries (Å, °) of (I)–(III).

The crystallographic data together with the atom-labelling scheme are given in Fig. 3 for (II) and in Fig. 4 for (III). Values for (II) (Faggiani *et al.*, 1977) and (III) (Lippert *et al.*, 1978) are taken from the literature.

	(I)	(II)	(III)
Pt···Pt(intradimer)	Pt1···Pt2 3.0421 (4)	Pt···Pt^{i} 3.085 (1)	Pt1···Pt2 3.104 (1)
Pt···Pt(interdimer)	Pt1···Pt1^{ii} 3.6968 (6)	Pt···Pt^{iii} 4.578 (1)	Pt2···Pt2^{iv} 3.167 (1) Pt1···Pt2^{v} 3.443 (1)
Pt—N	Pt1—N1 2.027 (7) Pt1—N2 2.029 (6) Pt2—N3 2.040 (6) Pt2—N4 2.018 (6)	Pt—N2 2.02 (1) Pt—N1 2.01 (1)	Pt1—N1 2.05 (2) Pt1—N2 2.02 (2) Pt2—N3 2.04 (2) Pt2—N4 2.02 (2)
Pt—O	Pt1—O1 2.047 (5) Pt1—O2 2.046 (6) Pt2—O1 2.038 (6) Pt2—O2 2.053 (5)	Pt—O1 2.03 (1) Pt—O1^{i} 2.03 (1)	Pt1—O1 2.02 (1) Pt1—O2 2.04 (1) Pt2—O1 2.07 (1) Pt2—O2 2.06 (1)
N—Pt—N	N1—Pt1—N2 90.2 (3) N3—Pt2—N4 90.4 (3)	N2—Pt—N1 89.3 (6)	N1—Pt1—N2 88.0 (7) N3—Pt2—N4 90.0 (7)
N—Pt—O in *cis* positions	N1—Pt1—O1 95.3 (2) N2—Pt1—O2 95.1 (3) N3—Pt2—O1 94.9 (3) N4—Pt2—O2 95.1 (2)	N2—Pt—O1 94.9 (5) N1—Pt—O1^{i} 94.5 (5)	N1—Pt1—O1 97.5 (6) N2—Pt1—O2 92.6 (6) N3—Pt2—O1 95.6 (6) N4—Pt2—O2 93.5 (6)
N—Pt—O in *trans* positions	N1—Pt1—O2 174.4 (2) N2—Pt1—O1 174.0 (3) N3—Pt2—O2 174.4 (3) N4—Pt2—O1 174.0 (3)	N2—Pt—O1^{i} 176.1 (6) N1—Pt—O1 175.6 (6)	N1—Pt1—O2 175.9 (6) N2—Pt1—O1 174.5 (6) N3—Pt2—O2 175.6 (5) N4—Pt2—O1 170.5 (4)
O—Pt—O	O1—Pt1—O2 79.5 (2) O1—Pt2—O2 79.5 (2)	O1—Pt—O1^{i} 81.3 (4)	O1—Pt1—O2 81.9 (5) O1—Pt2—O2 80.6 (5)
Pt—O—Pt	Pt1—O1—Pt2 96.3 (2) Pt1—O2—Pt2 95.8 (2)	Pt—O1—Pt^{i} 98.6†	Pt1—O1—Pt2 98.8 (5) Pt1—O2—Pt2 98.5 (5)

Symmetry codes: (i) $1-x, 1-y, -z$; (ii) $\frac{1}{2}+x, \frac{1}{2}-y, -z$; (iii) $-x, 1-y, 1-z$; (iv) $1-x, -y, 1-z$; (v) $-x, -y, 1-z$. † This value was not reported in the original paper (Faggiani *et al.*, 1977), and was therefore calculated in *TEXSAN* (Molecular Structure Corporation, 2001).

[3.085 (1) Å] or (III) [3.104 (1) Å] for (III). Additional features are the smaller O—Pt—O/Pt—O—Pt angles and the larger N—Pt—N angles in (I) compared with the corresponding angles in (II) and (III) (see Table 2).

The dinuclear cations are related by the operation of a 2_1 screw axis and stack along the *a* axis to give a pseudo-one-dimensional platinum chain (see Fig. 5). Although the interdimer Pt···Pt distance [Pt1···Pt1^{i} 3.6968 (6) Å; (i) $x+\frac{1}{2}, -y+\frac{1}{2}, -z$] is relatively long, we conclude that a weak metal–metal interaction is, to some extent, promoted between the Pt^{II} centres, since the colours of compounds (I)–(III) seem to be correlated with their shortest interdimer Pt···Pt distances: Pt···Pt(interdimer) 4.578 (1) Å for the colourless nitrate salt (Fig. 3) > Pt···Pt(interdimer) 3.6968 (6) Å for the pale yellow perchlorate salt > Pt···Pt(interdimer) 3.167 (1) Å for the deep yellow carbonate salt (Fig. 4). The dimer–dimer association in (I) is also stabilized with two hydrogen bonds formed between the ammines and the O atoms of hydroxo bridges [N1···O2^{i} 2.947 (8) and N2···O1^{ii} 2.973 (9) Å; (i) $x+\frac{1}{2}, -y+\frac{1}{2}, -z$; (ii) $x+\frac{1}{2}, -y+\frac{1}{2}, -z$; see the details in Table 3]. These hydrogen-bonding geometries further support the validity of the *syn* orientation of bridging hydroxo ligands in (I), and is considered as one of the reasons why the exceptional bent form is stabilized in (I). As summarized in Table 3, the crystal packing is further stabilized with extensive hydrogen bonds formed between the cations and the anions, leading to the three-dimensional hydrogen-bonding networks in the crystal structure. Nevertheless, the O(hydroxo)—H···O(ClO_4^-) and N(ammine)—H···O(hydroxo) hydrogen bonds are effectively shorter and stronger than the N(ammine)—H···O(ClO_4^-) ones. In summary:

(i) the dimer cation forms relatively strong hydrogen bonds with the two neighbouring perchlorate anions (Figs. 1*a* and *b*),

(ii) these ion-pair aggregates form moderate N(ammine)—H···O(hydroxo) hydrogen bonds with one another to give a one-dimensional chain in Fig. 5 and

(iii) the interchain interactions comprise relatively weak N(ammine)—H···O(ClO_4^-) hydrogen bonds.

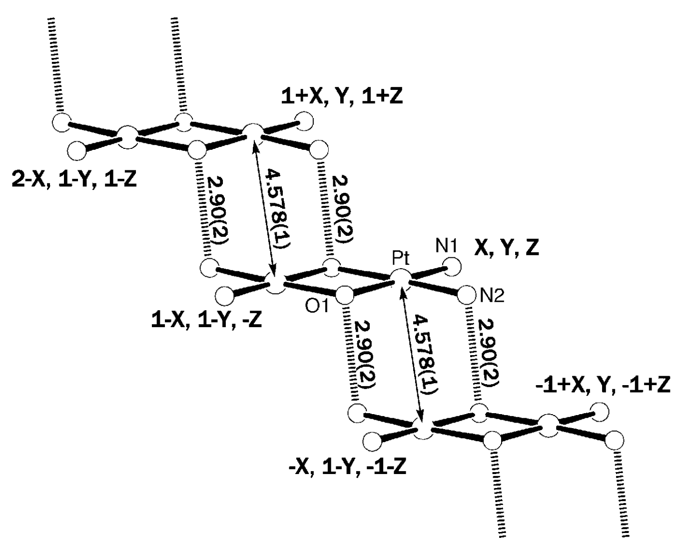

Figure 3
The stair-like dimer chain observed in $[Pt_2(NH_3)_4(\mu\text{-}OH)_2](NO_3)_2$ (II), where the crystal data are taken from the literature [Faggiani *et al.*, 1977; triclinic, space group $P\overline{1}$, *a* = 6.763 (12), *b* = 7.890 (18), *c* = 7.256 (13) Å, α = 92.3 (1), β = 133.1 (1), γ = 91.0 (1)°, *Z* = 1]. H atoms and nitrate anions are omitted for clarity. Dashed lines denote hydrogen bonds.

3.2. DFT investigations

Structures of the initial and the optimized geometries given for the

Table 3
Hydrogen-bonding geometry (Å, °) for (I).

D—H···A	D—H	H···A	D···A	D—H···A
O1···O4†			2.814 (9)	
O2···O8†			2.891 (8)	
N1—H1A···O2^{i}	0.89	2.10	2.947 (8)	158.4
N2—H2A···O1^{i}	0.89	2.09	2.973 (9)	170.7
N2—H2B···O5^{ii}	0.89	2.24	3.127 (11)	172.0
N4—H4A···O6^{iii}	0.89	2.32	3.178 (9)	161.5
N1—H1C···O8^{ii}	0.89	2.44	3.044 (8)	125.3
N4—H4B···O9	0.89	2.10	2.990 (9)	179.1
N3—H3A···O9^{iv}	0.89	2.46	3.007 (9)	120.1

Symmetry codes: (i) $\frac{1}{2}+x, \frac{1}{2}-y, -z$; (ii) $x-\frac{1}{2}, \frac{1}{2}-y, -z$; (iii) $\frac{3}{2}-x, -y, \frac{1}{2}+z$; (iv) $\frac{3}{2}-x, -y, z-\frac{1}{2}$. † H atoms on the hydroxyl ligands are not located.

five test cases are shown in Fig. 6. The SCF (self-consistent field) energies obtained for the five optimized geometries are summarized in Table 4. Selected interatomic distances and angles given for the optimized structures are also listed in Table 5. As shown in Fig. 6, geometry optimizations starting from the *pa* and *ba* conformers both gave the *pa* conformer as the energy-minimized structure, indicating that the planar skeleton is favourable when the H(hydroxo) atoms are located in an *anti* orientation. On the other hand, optimizations starting from the *ps*, *be* and *bx* conformers all gave the same structure corresponding to the *bx* conformer as the energy-minimized structure, where the dihedral angle between the Pt coordination planes within the dimer unit converged at 150.7 (1)°. This is quite consistent with the value observed in (I) [151.7 (1)°], even though the dimer cation in (I) does not have a *bx* form, but has a *be* form. Moreover, the latter three calculations reveal that the bent skeleton is preferable when the H(hydroxo) atoms are oriented in a *syn* fashion (note that either *endo* or *exo* is considered as *syn*). The two energy-minimized conformers are only slightly different in energy; the optimized conformer *bx* is 14.57 kJ mol^{-1} lower in energy than the *pa* one (see Table 4), indicating that the bent structure is essentially more stable in comparison with the planar one, at least, in the gaseous state.

3.3. Consideration for the planar-bent isomerism of the dimer cations in (II) and (III)

The orientation of H(hydroxo) atoms were not well determined in the previous reports for (II) and (III) (Faggiani *et al.*, 1977; Lippert *et al.*, 1978). However, the detailed investigations of their hydrogen-bonding interactions achieved in the crystal structure provide a clear description of the conformation with regard to the H(hydroxo) atoms in (II) and (III), as follows. As shown in Fig. 3 the dimer cations in (II) are arranged in a stair-like fashion to give a one-dimensional hydrogen-bonded array in which the shortest interdimer Pt···Pt distance is 4.578 (1) Å. The hydrogen-bonding geometry clearly shows that the dimer cation in (II) has an *anti* orientation.

On the other hand, Fig. 4 shows that a dimer of dimers is achieved in the crystal structure of (III), in which two dimers are correlated through an inversion centre, a single strong Pt···Pt interaction exists [Pt···Pt 3.167 (1) Å] within a tetranuclear aggregate, and the dimer–dimer association is also

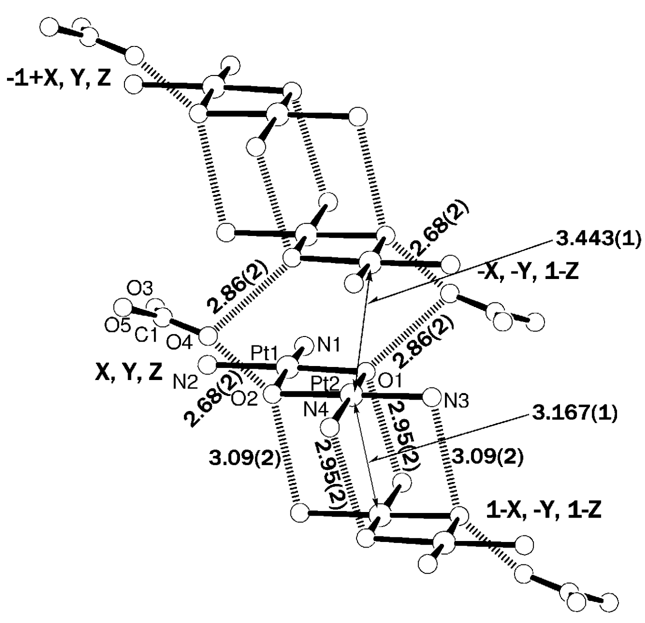

Figure 4
Pseudo-one-dimensional network of tetranuclear aggregates in $[Pt_2(NH_3)_4(\mu\text{-}OH)_2](CO_3)\cdot 2H_2O$ (III), where the crystal data are taken from the literature [Lippert *et al.*, 1978; monoclinic, space group $P2_1/c$, a = 7.127 (2), b = 11.416 (3), c = 15.379 (4) Å, β = 119.15 (1)°, Z = 4]. H atoms and water molecules are omitted for clarity. Dashed lines denote hydrogen bonds.

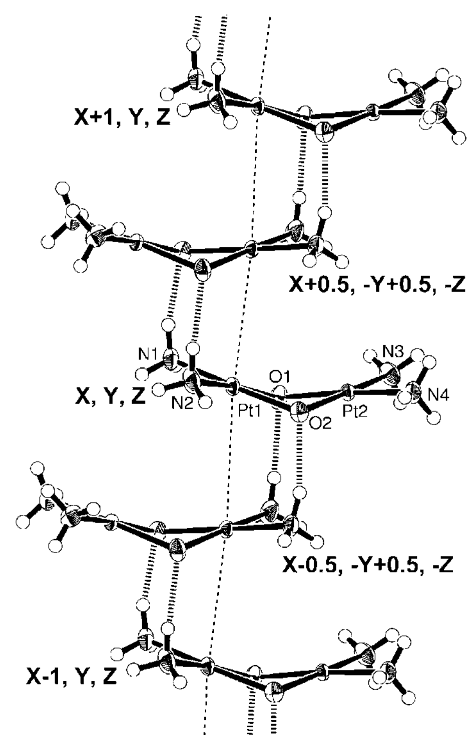

Figure 5
One-dimensional dimer chain in (I) growing along the *a* axis, where the dashed lines denote hydrogen bonds and the counterions are omitted for clarity.

Table 4
Summary for the geometry optimizations starting from the five possible conformers.

See experimental details in §2. Structures on the same calculations are shown in Fig. 6. Hinge angle: the tilt angle between the two Pt coordination planes within the dinuclear unit. The values have been calculated using *TEXSAN* (Molecular Structure Corporation, 2001). Values in parentheses correspond to the standard uncertainties estimated in the mean-plane calculations.

Initial conformation	Optimized conformation	Hinge angle (°)	SCF energy (kJ mol^{-1})	Relative difference in energy (kJ mol^{-1})
pa	*pa*	179.854 (3)	−1616853.599	14.57
ps	*bx*	150.714 (3)	−1616868.166	0.0
ba	*pa*	179.449 (3)	−1616853.598	14.57
be	*bx*	150.656 (3)	−1616868.166	0.0
bx	*bx*	150.788 (3)	−1616868.166	0.0

Table 5
Optimized geometries afforded by the five calculations listed in Table 4.

Distances and angles have been calculated using *TEXSAN* (Molecular Structure Corporation, 2001).

	pa → *pa*	*ps* → *bx*	*ba* → *pa*	*be* → *bx*	*bx* → *bx*
Pt1···Pt2	3.199	3.110	3.198	3.110	3.110
Pt1—N5	2.085	2.080	2.085	2.080	2.080
Pt1—N6	2.085	2.080	2.085	2.080	2.080
Pt2—N7	2.085	2.080	2.085	2.080	2.080
Pt2—N8	2.085	2.080	2.085	2.080	2.080
Pt1—O3	2.083	2.085	2.083	2.085	2.085
Pt1—O4	2.083	2.085	2.083	2.085	2.085
Pt2—O3	2.083	2.085	2.083	2.085	2.085
Pt2—O4	2.083	2.085	2.083	2.085	2.085
N5—Pt1—N6	93.86	95.12	93.88	95.16	95.14
N7—Pt2—N8	93.86	95.20	93.87	95.15	95.15
N5—Pt1—O3	93.28	92.29	93.17	92.23	92.25
N6—Pt1—O4	93.22	92.24	93.31	92.27	92.28
N7—Pt2—O3	93.28	92.23	93.18	92.24	92.25
N8—Pt2—O4	93.22	92.22	93.31	92.28	92.27
N5—Pt1—O4	172.8	172.1	172.7	172.0	172.0
N6—Pt1—O3	172.8	172.0	172.9	172.0	172.0
N7—Pt2—O4	172.8	172.0	172.7	172.0	172.0
N8—Pt2—O3	172.8	172.0	172.9	172.0	172.0
O3—Pt1—O4	79.66	80.22	79.67	80.20	80.19
O3—Pt2—O4	79.66	80.22	79.67	80.20	80.19
Pt1—O3—Pt2	100.34	96.47	100.33	96.46	96.50
Pt1—O4—Pt2	100.34	96.45	100.33	96.46	96.50
H-atom geometry given in a compact format					
N—H	1.027–1.029	1.027–1.029	1.027–1.029	1.027–1.029	1.027–1.029
O—H	0.981	0.982	0.981	0.982	0.982
Pt—O—H	113.9–114.0	114.6–114.7	113.8–114.1	114.7	114.7
Pt—Pt—O—H	122	121	122	121	121

supported by four hydrogen bonds formed between the ammines and the O atoms of hydroxo bridges. The hydrogen-bonding geometry clearly indicates that the H(hydroxo) atoms are oriented towards the outside of the tetranuclear aggregate. As shown in Fig. 4, two carbonate ions link the two neighbouring tetranuclear aggregates *via* relatively strong hydrogen bonds formed between the H(hydroxo) atoms and the O atoms of carbonates [O(hydroxo)···O(carbonate) 2.86 (2) and 2.68 (2) Å; Lippert *et al.*, 1978]. These clearly show that the dimer cation in (III) has a *syn* orientation in spite of the nearly planar geometry.

4. Conclusions

We have for the first time observed a bent form of the $[Pt_2(NH_3)_4(\mu\text{-}OH)_2]^{2+}$ cation in which the H(hydroxo) atoms have a *syn* orientation owing to the one-dimensional hydrogen-bonding network. Our DFT investigations reveal that the planar-bent selection could be given by the *anti–syn* selection at the H(hydroxo) atoms. Nevertheless, the carbonate salt shows that the *syn* orientation does not always lead to the bent form of the diplatinum core. In conclusion, the conformation of the $[Pt_2(NH_3)_4(\mu\text{-}OH)_2]^{2+}$ cation is primarily governed by the overall balance in the stability of crystal packing.

This work was supported by Grants-in-Aid for Scientific Research on Priority Areas (Nos. 10149248, 11136246 and 12023247 'Metal-assembled Complexes') from the Ministry of Education, Culture, Sports, Science and Technology of Japan. This work was partly supported by a Grant-in-Aid for Scien-

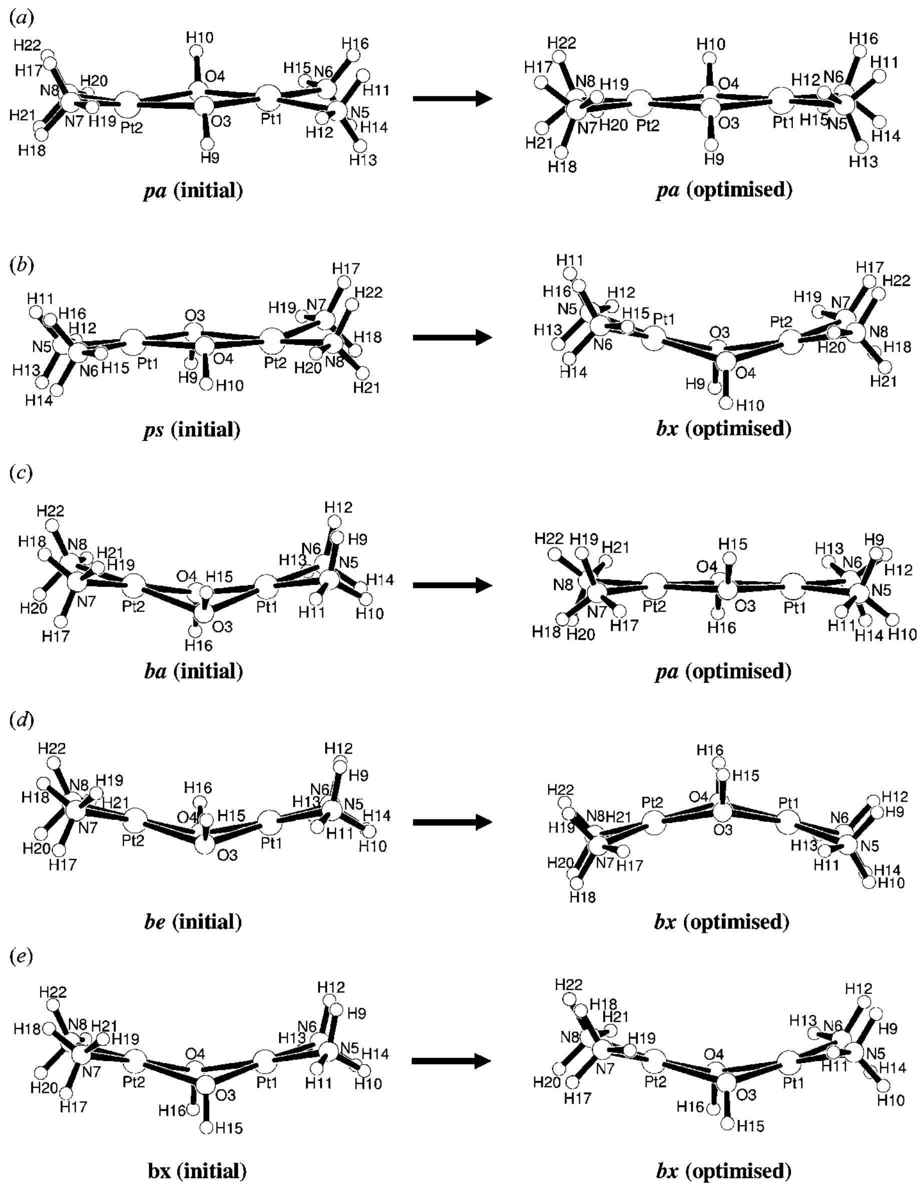

Figure 6
Structures of optimized geometries given from the five possible initial structures: (*a*) *pa* → *pa*; (*b*) *ps* → *bx*; (*c*) *ba* → *pa*; (*d*) *be* → *bx*; (*e*) *bx* → *bx*, where the conformers before and after each arrow respectively correspond to the initial and the optimized structures in each optimization.

tific Research (B) (No. 14340223) from the Ministry of Education, Culture, Sports, Science and Technology of Japan.

References

Aullón, G., Lledós, A. & Alvarez, S. (2000). *Inorg. Chem.* **39**, 906–916.

Aullón, G., Ujaque, G., Lledós, A., Alvarez, S. & Alemany, P. (1998). *Inorg. Chem.* **17**, 2971–2975.

Becke, A. D. (1993). *J. Chem. Phys.* **98**, 5648–5652.

Bruker (2001). *SAINT* (Version 6.22) and *SMART* (Version 5.625). Bruker AXS Inc., Madison, Wisconsin, USA.

Dunning, T. H. Jr & Hay, P. J. (1976). *Modern Theoretical Chemistry*, edited by H. F. Schaefer III. New York: Plenum Press.

Faggiani, R., Lippert, B., Lock, C. J. L. & Rosenberg, B. (1977). *J. Am. Chem. Soc.* **99**, 777–781.

Flack, H. D. (1983). *Acta Cryst.* A**39**, 876–881.

Frisch, M. J. *et al.* (1998). *Gaussian*98, Revision A.6. Gaussian, Inc., Pittsburgh, PA.

Hay, P. J. & Wadt, W. R. (1985*a*). *J. Chem. Phys.* **82**, 270–283.

Hay, P. J. & Wadt, W. R. (1985*b*). *J. Chem. Phys.* **82**, 299–310.

Jamieson, E. R. & Lippard, S. J. (1999). *Chem. Rev.* **99**, 2467–2498.

Johnson, C. K. (1976). *ORTEP*II. Report ORNL-5138. Oak Ridge National Laboratory, Tennessee, USA.

Lee, C., Yang, W. & Parr, R. G. (1988). *Phys. Rev. B*, **37**, 785–789.

Lippert, B., Lock, C. J. L., Rosenberg, B. & Zvagulis, M. (1978). *Inorg. Chem.* **17**, 2971–2975.

Molecular Structure Corporation (2001). *TEXSAN*, Version 1.11r1. MSC, 3200 Research Forest Drive, The Woodlands, TX 77381, USA.

Sakai, K. (2002). *KENX*. Graphical User Interface for *SHELXL*97. Tokyo University of Science, Japan.

Sakai, K., Ishigami, E., Konno, Y., Kajiwara, T. & Ito, T. (2002). *J. Am. Chem. Soc.* **124**, 12088–12089.

Sakai, K., Takeshita, M., Tanaka, Y., Ue, T., Yanagisawa, M., Kosaka, M., Tsubomura, T., Ato, M. & Nakano, T. (1998). *J. Am. Chem. Soc.* **120**, 11353–11363.

Sheldrick, G. M. (1996). *SADABS*. University of Göttingen, Germany.

Sheldrick, G. M. (1997). *SHELXS*97 and *SHELXL*97. University of Göttingen, Germany.

Wadt, W. R. & Hay, P. J. (1985). *J. Chem. Phys.* **82**, 284–298.